Madelung's Deformity

25

M. Claire Manske, Michelle A. James, and H. Relton McCarroll

Introduction

Madelung's deformity is an uncommon congenital wrist condition characterized by premature closure of the volar-ulnar aspect of the distal radius physis, volar carpal subluxation, and distal ulna prominence (Fig. 25.1). It is classified as a malformation of the radio-ulnar axis involving the entire upper limb, according to the Oberg-Manske-Tonkin Classification [1]. It accounts for less than 2% of congenital upper extremity differences [2]. Madelung's deformity is most commonly idiopathic, but a Madelung-like deformity may result from trauma, infection, multiple hereditary exostoses (MHE), and Ollier's disease. Additionally, it is associated with skeletal dysplasias involving mutations of the short stature homeobox (SHOX) gene. Madelung's deformity predominantly affects females and becomes clinically apparent during adolescence. Affected individuals may present with wrist pain, restricted range of motion of the wrist and forearm, decreased grip strength, and function difficulties, as well as aesthetic concerns. Several surgical options have been described for children with Madelung's deformity, depending on their age and degree of deformity, and include physiolysis, soft tissue release, and osteotomies, with promising outcomes.

History

The first description of Madelung's deformity is attributed to Dupuytren in 1834. Although not the first to identify the wrist deformity that now bears his name, the German surgeon Otto Madelung was the first to provide a comprehensive clinical description of "manus valga," as well as its proposed etiology and treatment options [3–5]. At the Congress of the German Society for Surgery in Berlin in 1878 and in subsequent publications, Madelung presented a case series of patients in whom "the distal end of the ulna juts out clearly. The styloid process and articular surface are recognizable and become apparent by feel. The hand, for itself alone regarded, is normal, but it has dropped forward. The widest diameter of the wrist is increased by almost double…The whole lower epiphysis of the radius of the deformed side is also angulated volarwards" [6, 7]. Madelung described this condition as commonly bilateral and predominantly affecting females who usually presented in early adolescence [7]. Although his clinical observations predated the availability of radiographs, Madelung's descrip-

M. C. Manske · M. A. James (✉) · H. R. McCarroll
Pediatric Hand and Upper Extremity Surgery, Department of Orthopedic Surgery, Shriners Hospitals for Children—Northern California, Sacramento, CA, USA

University of California Davis School of Medicine, Sacramento, CA, USA
e-mail: mjames@shrinenet.org

D. R. Laub Jr. (ed.), *Congenital Anomalies of the Upper Extremity*,
https://doi.org/10.1007/978-3-030-64159-7_25

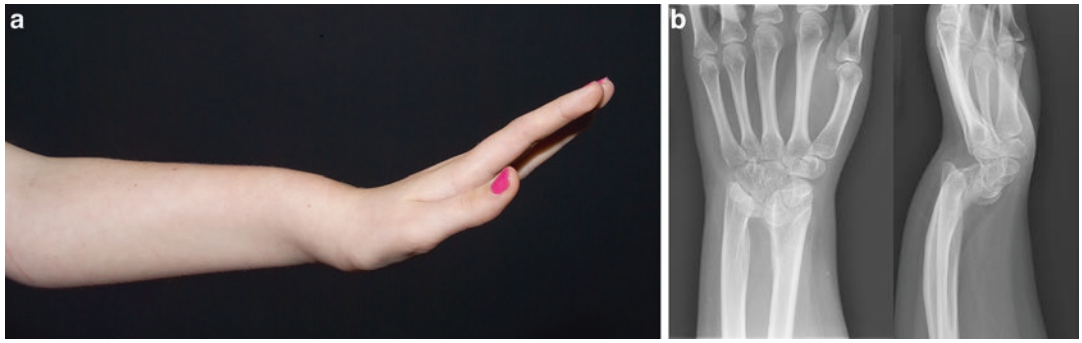

Fig. 25.1 (**a**) Clinical photograph and (**b**) AP and lateral wrist radiographs of patient with Madelung deformity. (Copyright Shriners Hospitals for Children—Northern California)

tion remains accurate today and is supported by subsequent radiographic and epidemiologic studies.

Anatomy and Etiology

The etiology of Madelung's deformity is unknown. The pathologic finding characteristic of Madelung's deformity is premature arrest of the volar-ulnar aspect of the distal radius physis, but the mechanism by which this physeal arrest occurs is incompletely understood. Both ligamentous and osseous abnormalities have been identified, but it has yet to be demonstrated which is the primary pathoanatomy and which occur secondarily. In 1992, Vickers and Nielsen described an aberrant ligament between the lunate and the volar aspect of the distal radius observed in 91% of individuals with Madelung's deformity [8, 9]. Although histologically normal, this ligament is abnormally thick and originates on the radial metaphysis, rather than the epiphysis. The authors proposed that this ligament, known as "Vickers ligament," tethers the lunate in a proximal position between the radius and ulna which in turn causes compression of the volar-ulnar epiphysis and physis of the distal radius and inhibits longitudinal growth. Munns et al. evaluated the histopathology of the distal radius physis in patients with Madelung's deformity and identified disordered physeal anatomy of the distal radius, including disruption of the normal columnar arrangement of mature chondrocytes, expansion of the hypertrophic layer, reduction of the proliferative zone, and presence of hypertrophic osteoid in the metaphysis, suggesting impaired endochondral ossification [10, 11].

Although the genetic basis of Madelung's deformity is not clear, pedigree studies suggest an autosomal dominant inheritance pattern with variable expressivity and penetrance [12]. Moreover, the presence of Madelung's deformity in syndromes related to deficiency of the short stature homeobox (SHOX) gene syndromes, including Leri-Weill dyschondrosteosis [13], Turner's syndrome [13, 14], and Langer mesomelic dysplasia [15], provides potential insight into the pathogenesis. The SHOX gene, located on the pseudo-autosomal region of the sex chromosomes, is expressed in both males and females and is thought to play a role in bone growth and development [13, 16]. Haploinsufficiency of the SHOX gene results in Leri-Weill dyschondrosteosis (LWD), a dominantly inherited skeletal dysplasia presenting with short stature and mesomelic limb shortening; Madelung deformity is observed in 74% of individuals with LWD [13]. Madelung's deformity is also seen in association with Langer mesomelic dysplasia (LMD), which results from a homozygous or compound heterozygous mutation of the SHOX gene and is characterized by severe short stature and both rhizomelic and mesomelic shortening; Madelung's deformity is seen less commonly with LMD than LWD. Turner's syndrome, a mesomelic skeletal dys-

plasia resulting from the combination of SHOX haploinsufficiency and a 45 X,O karyotype, is characterized by short stature, ovarian failure, and a variety of somatic features, including webbed neck, lymphedema, cardiac and renal abnormalities, and skeletal defects; Madelung's deformity is observed in 7% of those with Turner's syndrome [13, 16]. The variable prevalence of Madelung deformity in these SHOX deficiency syndromes is not entirely understood but may result from the interaction of SHOX mutations and estrogen [17]. This interaction with sex steroids may also explain the female predilection and presentation during the adolescent growth spurt. Madelung's deformity has also been reported in association with pseudohypoparathyroidism types 1a and 1b resulting from GNAS gene mutations [18, 19] and nail-patella syndrome [20], which highlights the complexity of the genetic basis of Madelung's. Further research is needed to delineate the genetic mutations associated with Madelung's deformity.

Madelung-like deformities due to post-traumatic distal radius physeal arrest (Fig. 25.2), post-infection, sickle cell disease, or gymnast wrist (physeal arrest due to repetitive axial loading of the wrist) are distinguished by patient history. Other skeletal dysplasias such as multiple hereditary exostoses and Ollier's disease may also result in a Madelung-like deformity, but these are differentiated by the presence of systemic bone changes. A reverse Madelung's deformity may also present with wrist deformity, pain, and limited forearm motion. Wrist and forearm radiographs will distinguish this diagnosis, in which the distal radial articular surface is angulated dorsally, dorsal subluxation of the carpus, volar displacement of the distal ulna, and dorsal bowing of the radial shaft (Fig. 25.3). It is not clear that this rare deformity is related to Madelung's deformity.

Diagnosis

The diagnosis of Madelung's deformity is made based on clinical and radiographic findings.

Clinical Presentation

Individuals with Madelung's deformity are commonly female (4:1 female-to-male ratio) and present in their pre-teen or adolescent years [21]. Typically, the chief complaint relates to the appearance of the wrist, which may have been initially subtle but has worsened with skeletal growth. This deformity is characterized by a volar-ulnar tilt of the radius due to the abnormalities of the distal radial physis. Because the ulna is unaffected, it grows normally, often longer than the radius and assumes a dorsally subluxated position. Additional concerns include wrist pain, stiffness, and difficulties with activities of daily living or recreational activities. Family history may be remarkable for other affected family members (especially females), and younger sib-

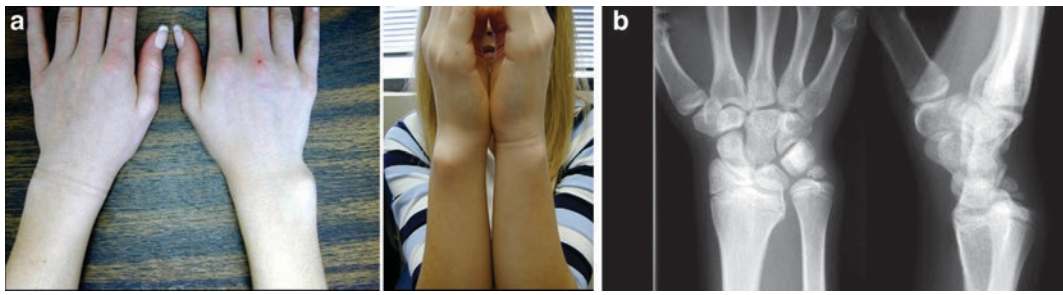

Fig. 25.2 (**a**) Clinical photographs and (**b**) PA and lateral wrist radiographs of a patient with post-traumatic Madelung's deformity from a traumatic injury to the volar ulnar physis of the distal radius. (Copyright Shriners Hospitals for Children—Northern California)

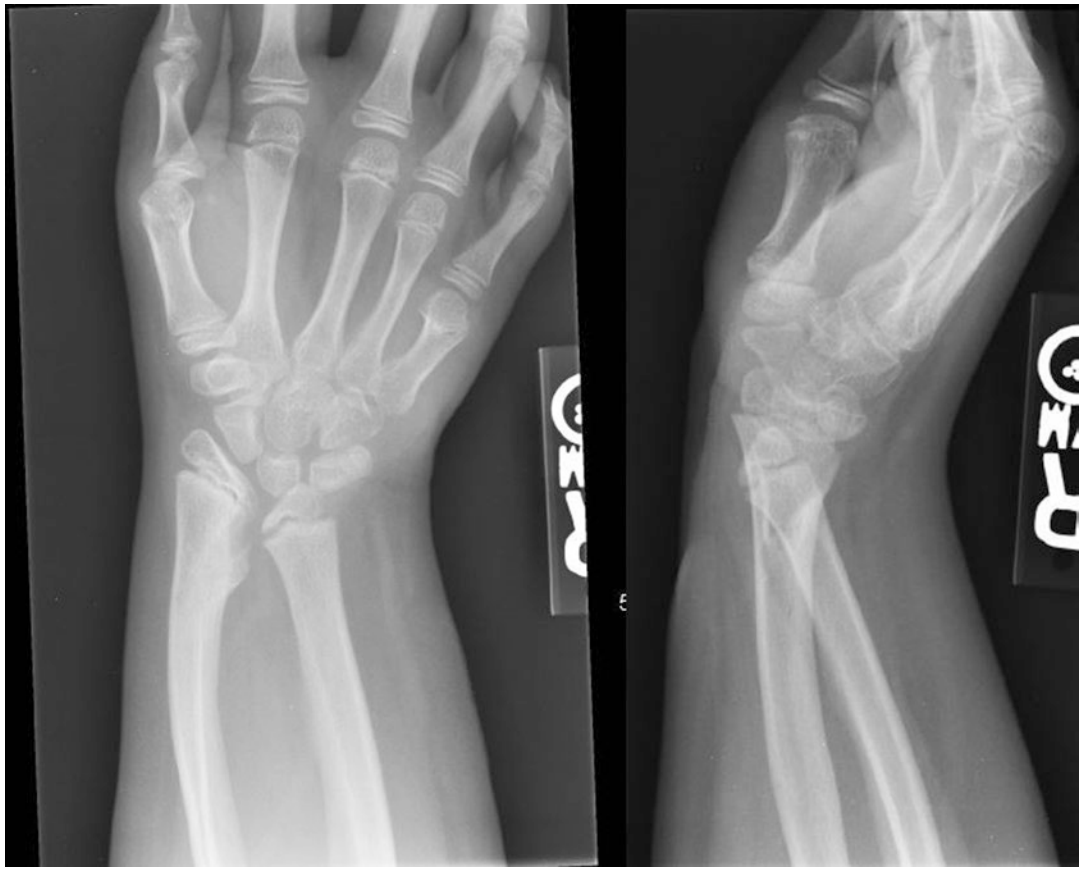

Fig. 25.3 PA and lateral radiographs of a reverse Madelung's deformity with dorsal angulation of the distal radius physis, dorsal subluxation of the carpus, and volar displacement of the distal ulna. (Copyright Shriners Hospitals for Children—Northern California)

lings should be examined (including wrist radiographs) to identify subtle abnormalities prior to the onset of symptomatic deformity.

Physical examination is notable for a prominent distal ulna with volar subluxation of the carpus relative to the forearm (volar sag) and forearm shortening and palmar curvature (see Fig. 25.1). Affected individuals may have limited range of motion (particularly in forearm supination and wrist extension), reduced grip strength, and DRUJ instability. Typically hand and finger function is unaffected, although attritional rupture of the extensor tendons has been reported due to the dorsal prominence of the ulna in long-standing deformity [22–24]. Seventy-four percent of affected individuals have bilateral deformity which may be asymmetric [20]. Children should also be evaluated for short stature, neck webbing, short metacarpals, and other clinical findings associated with SHOX deficiency and referred for genetic assessment if present.

Radiographs of the wrist and forearm confirm the diagnosis of Madelung's deformity. Wrist x-rays demonstrate physeal closure of the volar-ulnar aspect of the distal radius, lunate subsidence ("carpal pyramidalization"), volar bowing of the radial shaft, and dorsal subluxation of the distal ulna. Numerous radiographic measurements have been described to quantify Madelung's deformity. Although initial parameters were based

on the radius, the radiographic criteria based on the ulna have been shown to be more reliable given the anatomic variability of the radius. McCarroll et al. evaluated five radiographic parameters to quantify Madelung's deformity and found that ulnar tilt, lunate subsidence, and palmar carpal displacement most reliably and reproducibly quantify the severity of Madelung's deformity [25] (Fig. 25.4). In a subsequent study, McCarroll et al. established threshold values for these radiographic findings to diagnose Madelung's deformity: ulnar tilt ≥33°, lunate fossa angle ≥40 °, lunate subsidence ≥4 mm, or palmar carpal displacement of ≥20 mm [26]. Zebala et al. recognized that up to one-third of individuals with Madelung's demonstrate proximal forearm deformity in addition to the wrist deformity; this includes increased sagittal bow of the radial diaphysis, decreased radial length, and increased radial head-capitellum distance [27]. Recognition of proximal deformity on full-length forearm x-rays is important as proximal involvement influences treatment and outcomes.

Magnetic resonance imaging (MRI) and computed tomography (CT) are typically not required to diagnose Madelung's deformity, although they may be useful for treatment planning in early or complex cases. MRI may be useful to evaluate to assess the location and extent of physeal disease and identify Vickers ligament in young children with mild deformity in whom physiolysis and Vickers ligament excision is being considered. With advances in three-dimensional modeling for surgical planning, CT scans may become increasingly useful to delineate the complex three-dimensional deformity of Madelung's deformity and reveal previously unidentified anatomic findings. Paymani et al. [28] reported the anatomic findings on three-dimensional CTs in 28 wrists with Madelung's deformity and identified abnormalities of the lunate fossa and difference in intracarpal angles compared to unaffected wrists, in addition to confirming radiographic findings (increased ulnar tilt, lunate subsidence, lunate fossa angle, and palmar carpal displacement) associated with Madelung's. Moreover, three-dimensional modeling using CT scans is in the early phases of development for surgical planning in the correction of complex deformity.

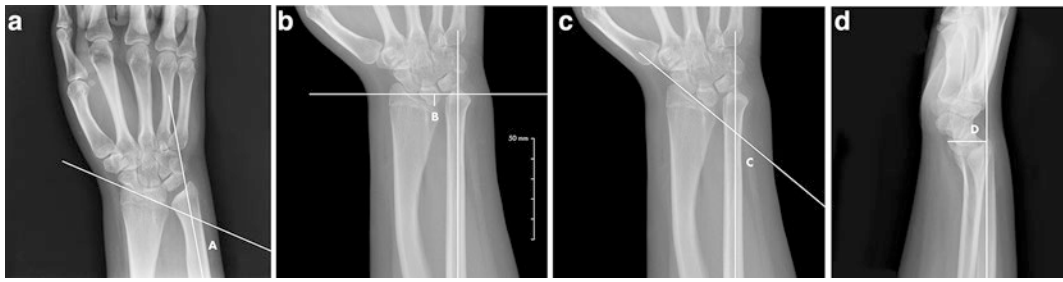

Fig. 25.4 Radiographic parameters of Madelung deformity. (**a**) (Ulnar tilt): Ulnar tilt is defined on the PA x-ray as the complement (90°-angle A) of the acute angle (angle A) between the longitudinal axis of the ulna and a line tangential to the proximal surfaces of the scaphoid and lunate. (**b**) (Lunate subsidence): Lunate subsidence on a PA x-ray is defined as the distance in millimeters (distance B) between the most proximal point of the lunate and a line perpendicular to the longitudinal axis of the ulna and through its distal articular surface. The measurement is positive if the ulna extends distal to the proximal surface of the lunate. (**c**) (Lunate fossa angle): Lunate fossa angle on a PA x-ray is defined as the complement (90°-angle C) of the acute angle (angle C) between the longitudinal axis of the ulna and a line across the lunate fossa of the radius. (**d**) (Palmar carpal displacement): Palmar carpal displacement on a lateral x-ray is defined as the distance in millimeters (distance D) between the longitudinal axis of the ulna and the most palmar point on the surface of the lunate or capitate. Copyright Shriners Hospitals for Children—Northern California

Treatment

The optimal treatment of Madelung's deformity remains controversial. Factors influencing treatment decisions include skeletal age, deformity severity, and symptoms. Nonoperative treatment is indicated in children with asymptomatic deformity or mild intermittent symptoms. These children may be monitored with serial radiographs at 6- to 12-month intervals. This is often appropriate for younger siblings of affected individuals who are identified prior to the onset of symptoms or substantial deformity. However, those with mild deformity at a young age may be indicated for surgery to prevent deformity progression. Other indications for operative intervention include pain, functional limitations, or progressive or unacceptable deformity.

Surgical treatment of Madelung deformity can be divided into three categories: early prevention, late correction, and salvage procedures in adulthood. Early prevention is indicated in young, skeletally immature children and consists of physiolysis and Vickers ligament release. Late correction, consisting of radius and ulna osteotomies to correct established deformity, may be considered in older children and adolescents with limited growth remaining. Lastly, salvage procedures, including partial or complete wrist arthrodesis, resection arthroplasty, or staged osteotomy with implant arthroplasty, may be considered in the setting of radiocarpal or DRUJ arthritis [17]. This chapter will focus on the early prevention and late correction procedures performed in childhood and adolescents.

Physiolysis and Vickers Ligament Release

Physiolysis and Vickers ligament release are indicated in young patients with minimal deformity and substantial growth remaining. The goal of the procedure is to restore radial growth and carpal alignment. The procedure was originally described using a transverse wrist incision [8], but modifications of this procedure utilize a longitudinal incision [29, 30].

The procedure is performed under tourniquet control and with a regional nerve block of the extremity. A traditional Henry approach to the volar distal radius along the flexor carpi radialis (FCR) is utilized. Vickers ligament is identified deep to the pronator quadratus on the distal ulnar border of the volar radius, elevated from proximal to distal, and excised to release the soft tissue tether. The bone bridge on the volar-ulnar aspect of the distal radial physis is identified, using preoperative imaging, intraoperative fluoroscopy, and direct inspection. A curette, rongeur, or burr is used to resect the bone bridge until the normal appearing physeal cartilage (blue coloration) is identified; care must be taken to avoid injury to the adjacent healthy physis. Fat or pronator quadratus muscle is interposed into the bone defect to decrease the risk of physeal bar recurrence. The pronator is then repaired and the skin closed in layers. The wrist is immobilized in a short arm cast for 2 weeks (Fig. 25.5). Formal therapy is not typically needed to regain wrist range of motion. Postoperatively, wrist radiographs are obtained at 6-month intervals to monitor for restoration of radial growth. If the ulna appears to be overgrowing, epiphysiodesis should be considered.

In their original description of the surgical technique, Vickers and Nielsen reported the outcomes of ligament release and physiolysis in 11 skeletally immature patients (15 wrists) [8]. All patients reported improvement in wrist pain, four of whom had complete resolution. No patients had progression of their wrist deformity, and slight improvement was observed in most cases. Forearm supination improved by a mean of 23°, but this improvement was not sustained at long-term follow-up. More recently, Otte et al. reported the outcomes of this procedure in 6 skeletally immature females (12 wrists) at a mean age of 7.5 years [31]. At final follow-up (minimum 17 months), the radial physeal angle improved in 10 of the 12 wrists (mean of 7.5 degrees of improvement), and metaphyseal growth was observed in 11 of the 12 wrists. All patients had postoperative resolution of their pain postoperatively, but two reported intermittent pain at final follow-up. All were able to return to their

Fig. 25.5 AP wrist radiograph before and 2 months after Vickers ligament release and physiolysis. (Copyright Shriners Hospitals for Children—Northern California)

preoperative level of activity. Del Core and colleagues [32] reported the long-term outcomes of this procedure into young adulthood. At a mean 10 years follow-up, six of the eight wrists were completely pain free, and forearm and wrist range of motion at long-term follow-up were similar to preoperative values. Radiographically, ulnar tilt and palmar carpal displacement did not change substantially compared to preoperative values, but lunate subsidence progressed. Based on these studies, it appears that this procedure results in pain relief in most patients, preservation of motion, and possible restoration of longitudinal growth. Whether it prevents deformity progression has not been clearly demonstrated.

Radial Dome Osteotomy

In older children with limited growth potential, established deformity, and pain or functional limitations, boney procedures are indicated. A dome osteotomy of the radius corrects the deformity in both the sagittal and coronal plane and is often performed concomitantly with a distal ulna epiphysiodesis or ulnar shortening osteotomy, discussed subsequently.

Under general anesthesia with an upper extremity tourniquet, a standard Henry approach to the distal radius is performed. Vickers ligament may be released as described above. The metaphyseal-diaphyseal junction is identified, and the periosteum is elevated circumferentially and retracted with small Hohmann retractors in preparation for the osteotomy. A small stab incision is made at the tip of the radial styloid, and the dorsal sensory branch of the radial nerve is protected. Two parallel or divergent 0.062 inch K-wires are placed on the styloid and driven retrograde into the distal radius, short of the osteotomy site. Because the distal fragment will be rotated, the K-wires should be placed nearly longitudinally to ensure that they will capture the proximal fragment after the correction. Under fluoroscopic

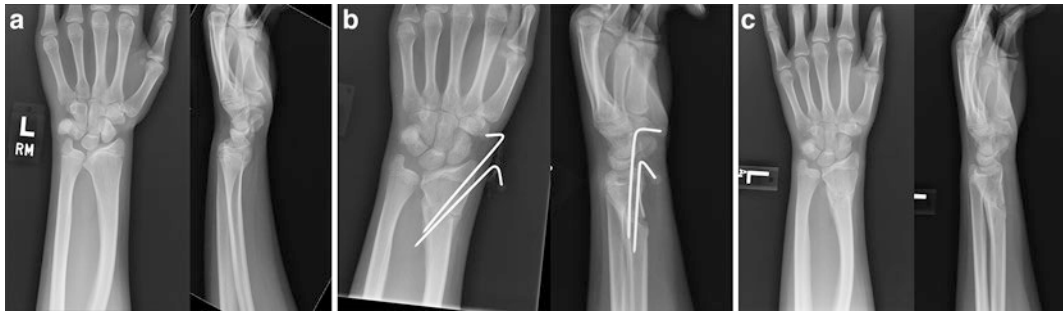

Fig. 25.6 Correction of Madelung deformity via distal radius dome osteotomy. (**a**) Preoperative radiographs. (**b**) Postoperative radiographic appearance, immediately before pin removal. (**c**) Final radiographic appearance at 3 months after surgery. (Copyright Shriners Hospitals for Children—Northern California)

guidance and direct visualization, a dome-shaped osteotomy is performed at the level of the metaphysis, proximal enough to avoid injury to the DRUJ and, if open, the distal radius physis. The osteotomy may be performed with a Domesaw® (Matric Orthopaedics, Inc., Twin Falls, ID) or by using a K-wire to perforate the volar and dorsal cortex several times in a crescent shape and connecting the perforations with an osteotome. The osteotomy should be concave in both the coronal and sagittal planes to allow multiplanar deformity correction. It is the authors' preference to perform the osteotomy with the concave portion of the dome distal (i.e., a smile, not a frown), as a convex osteotomy creates a prominent metaphyseal spike on the distal fragment that limits radial deviation and extension. Longitudinal traction and manual manipulation are used to radially deviate, extend, and dorsally translate the distal fragment to correct the deformity. If necessary to achieve the desired correction, a spike of bone may be removed from the proximal volar cortex, which may be used as a bone graft in the osteotomy site. The previously placed K-wires are then driven across the osteotomy site into the proximal fragment with bicortical purchase (see Fig. 25.5). The pins are cut and bent outside the skin. In children with a large degree of correction or prolonged tourniquet time, we recommend performing a fasciotomy of the volar forearm. The skin is closed in layers, and a well-padded long-arm splint or bivalved cast is applied. The pins are removed in clinic when radiographic healing is evident, typically between 4 and 8 weeks. Range of motion exercises is initiated when the pins are removed, and a removable wrist splint is worn for activity and weaned over 2 weeks as comfort allows (Fig. 25.6).

Reported outcomes of the dome osteotomy are encouraging. Harley et al. [33] reported that children treated with dome osteotomy and volar ligament release reported improved wrist pain and appearance and increased forearm supination and wrist extension, without loss of pronation or wrist flexion at a mean 2-year follow-up. Additional ulnar-sided surgeries, either performed simultaneously or in a staged fashion, were common. Long-term studies of this procedure indicate sustained outcomes. The same cohort of children in the Harley study was evaluated in early adulthood at a mean of 11 years following surgery [34]. The authors note preservation of radial inclination but slight progression of lunate subsidence (2 mm). They observed no loss of wrist extension and forearm supination. Many patients had additional procedures following the dome osteotomy, most commonly ulnar shortening osteotomy; other procedures included revision dome osteotomy, Darrach resection, and Sauve-Kapandji procedure. Importantly, the authors identified an association between whole bone involvement as described by Zebala [27] and arthritic changes, as well as an association between arthritic changes and increasing (worse) disabilities of the arm, shoulder, and hand (DASH) scores, confirming that those with whole bone involvement have poorer radiographic and functional outcomes.

Distal Ulna Epiphysiodesis

A distal ulna epiphysiodesis is often performed in conjunction with the radial osteotomy in young patients who are at risk of worsening deformity due to continued ulnar growth. The distal ulnar physis is localized under fluoroscopy using a 25-gauge hypodermic needle. A small longitudinal incision on the ulnar border of the distal forearm is centered over the physis. Subperiosteal dissection is performed, and curettes or a small drill is introduced into the physis. The physis is ablated under fluoroscopic guidance. Because the distal ulnar physis tends to be robust, it can be difficult to ablate, and we are aggressive in removing all of the physeal cartilage. The skin is closed in layers with dissolvable suture, and a long arm cast is applied as above.

Ulnar Shortening Osteotomy

In children with limited growth remaining and positive ulnar variance in addition to the radius deformity, an ulnar shortening osteotomy is often performed in conjunction with the radius osteotomy. It should also be considered in skeletally mature individuals with Madelung's deformity and ulnar-sided wrist pain due to ulnocarpal abutment [35].

A longitudinal incision is made over the ulnar border of the mid and distal forearm with care to protect the dorsal sensory branch of the ulnar nerve. The interval between the extensor carpi ulnaris (ECU) and flexor carpi ulnaris (FCU) is developed in the mid forearm to expose the ulnar shaft. Subperiosteal exposure of the ulnar shaft is performed, and an appropriately size plate that will accommodate the osteotomy is selected; we usually use a 2.7-mm LCDC plate (DePuy Synthes, West Chester, PA), but 3.5-mm plates can be used for larger patients or stacked 1/3 tubular plates for smaller patients, as described by Waters and Bae [21]. The distal holes are drilled with partial placement of the screws. The osteotomy site is marked, as well as a longitudinal line along the plate to guide against malrotation. Two parallel oblique passes are made with a sagittal saw to correspond with the desired amount of shortening. In the authors' experience, it is difficult to shorten more than about 6 mm and still achieve bony apposition. The ring of bone is removed and the plate and screws reapplied. The osteotomy is reduced, and proximal fixation is achieved with the screw applied in compression. Fluoroscopic imaging and direct visualization are used to confirm the position of the implants and good bone contact. Fluoroscopic images of the wrist with the forearm in neutral rotation view are used to assess the ulnar variance after correction. The skin is closed in layers with dissolving suture. The arm is immobilized as needed for the radius osteotomy.

Very Distal Radius Osteotomy

The dome osteotomy of the radius is effective at addressing the radial bow and palmar tilt but is less effective at correcting the ulnar tilt. In cases in which the ulnar tilt is a major component of the deformity, a very distal dome osteotomy allows correction of the ulnar tilt as well as the radial bow and palmar tilt. Additionally, when there is substantial radial bow, the very distal radius osteotomy can be combined with a proximal radial shaft osteotomy.

The very distal osteotomy was described by McCarroll and James [36] (see Fig. 25.6). In this procedure, the ulna is prepared for a shortening osteotomy first. The ulna is approached, and a plate is provisionally attached distal to the osteotomy site as described previously. A transverse osteotomy is made with a sagittal saw, and the ends of the ulna are allowed to overlap. The mobility of the ulnar ends is necessary to allow the radius to mobilize freely. The distal radius is then approached dorsally from the carpometacarpal (CMC) joints to the outcropper muscles in the forearm. The third dorsal compartment is opened, the EPL liberated, and the extensor compartments elevated and retracted. The distal radius is exposed through a longitudinal incision in the periosteum, followed by a small capsulotomy made in the dorsal wrist capsule to assess the palmar tilt of the articular surface. A K-wire is placed, blunt end

first, in the joint to estimate the palmar tilt of the distal radius. A second K-wire is placed in the radial styloid transversely across in radius, just proximal to the dorsal joint surface. A T-plate is selected for the planned osteotomy; an outline of the plate is marked on the dorsal radial cortex with a surgical marking pen. We use a stainless steel buttress T-plate with three or four proximal holes for 3.5-mm screws. This plate is malleable and able to bend to the new contour of the radius. A guideline is then drawn across the dorsal radius parallel to the radius articular surface, which is placed as distally as possible but with sufficient space to place the T-plate. A second mark is drawn from the proximal margin of the DRUJ perpendicular to the axis of the radius. This is the location of the second osteotomy cut for the very distal osteotomy. A third line is drawn between the first two guidelines but at half the angle to the perpendicular line; this is the line of the first cut for the very distal osteotomy and will correct the ulnar tilt of the articular surface by 50%. The ulnar extent of the osteotomy must be proximal to the DRUJ. The osteotomy is made with a sagittal saw following the central guide mark in a radial-ulnar direction and parallel to the vertical joystick and the K-wire across the articular surface of the radius in a dorsal to palmar direction. The K-wires are then used as joysticks to correct the palmar and ulnar tilt of the distal fragment.

At this point, the hand, carpus, and distal radius are a separate, mobile fragment, which often cannot be positioned on the radial metaphysis without shortening the radius. A segment of the radius is resected from the proximal end of the osteotomy and is used to shorten the radius and allow the distal radius to be placed on radial metaphysis in the corrected alignment. If the distal osteotomy is acceptably aligned, only a transverse osteotomy of the radial shaft is needed; however, if addition correction is needed, the proximal osteotomy can be altered to achieve the desired correction. The end of the proximal radius fragment often has a very sharp dorsal point that provides poor support to the distal fragment, and sufficient bone must be removed to shorten the radial shaft appropriately and provide a flat stable surface to support the distal fragment. The osteotomy is provisionally fixed with K-wires.

Attention is turned back to the distal radius, and the final T-plate is selected. The plate is contoured to the shape of the corrected distal radius, and the plate is fixed to the distal radius with care to avoid penetration of the radiocarpal joint or DRUJ. The proximal screws of the T-plate are positioned proximal to the more proximal of the two osteotomies to achieve fixation of both osteotomies.

Attention returns to the ulnar shortening osteotomy. The previously selected ulnar plate is attached to the distal ulna via the previously drilled screw holes. Manual traction is applied to the distal ulna, and the overlap between the distal and proximal ulna is marked. A segment of ulna is removed from the end proximal to the osteotomy site to remove the overlap between the bone ends. The fragments are then aligned and the plate secured to the proximal fragment. The skin is closed with dissolvable suture in a layered fashion and the upper extremity placed in a well-padded, bivalved short arm cast. The cast is overwrapped at 1 week and removed at 6 weeks. Radiographs are obtained at 6 weeks, and the patient is transitioned to a removable wrist splint if there is clinical and radiographic evidence of healing. Serial x-rays are obtained at 4- to 6-week intervals until solid union is observed. The patient may then wean from the splint and increase upper extremity use and activities as tolerated (Fig. 25.7).

Short-term follow-up of 17 wrists treated with this procedure demonstrate reliable bony union in 6 weeks to 3 months and high patient satisfaction with the appearance of the wrist and resolution of pain. No patients developed infections or neurovascular compromise. The authors report that the procedure preserved DRUJ function while correcting the deformity. Larger and long-term follow-up studies are needed to further evaluate these outcomes.

Multiple Osteotomies Using Three-Dimensional Modeling

Historically, surgical planning for correction of Madelung's deformity was based on radiographs, which provides a two-dimensional representation of a complex three-dimensional deformity.

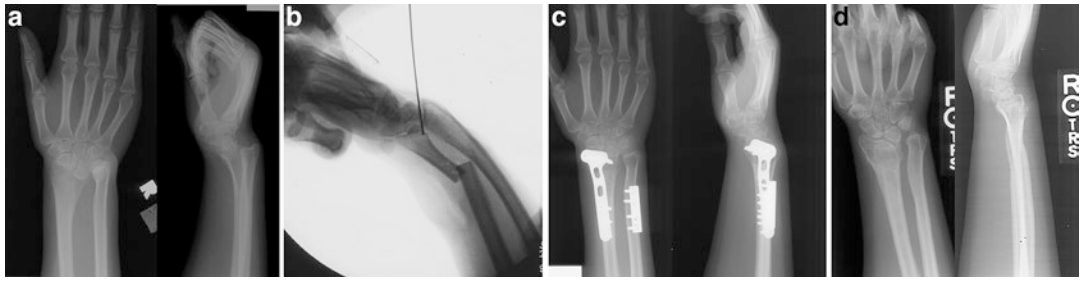

Fig. 25.7 Correction of Madelung deformity via very distal radius osteotomy. (**a**) Preoperative radiographs. (**b**) Intraoperative fluoroscopic image. The ulna has been cut and allowed to move into bayonet apposition. A K-wire has been inserted across the radiocarpal joint. (**c**) Postoperative radiographs at 6 months after surgery demonstrating healed osteotomies with hardware still in place. (**d**) Final postoperative radiographs 2 years after initial surgery, hardware has been removed. (Copyright Shriners Hospitals for Children—Northern California)

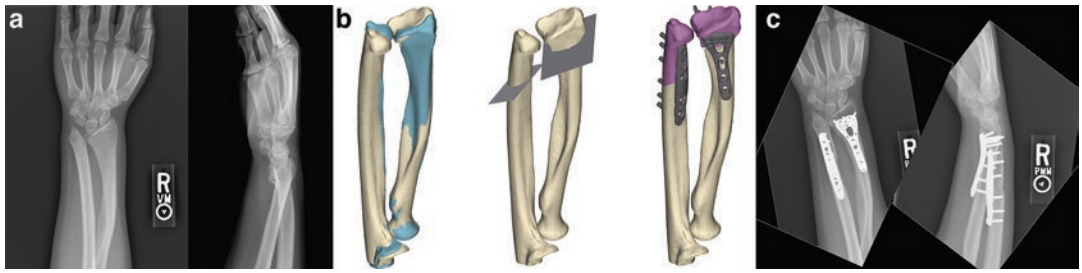

Fig. 25.8 Correction of Madelung deformity via multiple osteotomies using three-dimensional modeling. (**a**) Preoperative wrist radiographs. (**b**) Preoperative plan. The first image shows the preoperative state (in *white*) superimposed on a mirror image of the contralateral side (in *green*). Next, the planned osteotomy sites are indicated. Lastly, the planned outcome with hardware in place; corrected distal fragments in *purple*. (**c**) Final radiographic appearance at 4 months after surgery. (Copyright Shriners Hospitals for Children—Northern California)

Technological advances in CT imaging and computer programming now allow a more comprehensive three-dimensional understanding of Madelung's deformity and enable comparison to the contralateral extremity or to an age-matched normal limb. Additionally, this technology assists the surgeon in accurately planning and performing three-dimensional osteotomies using three-dimensional printed, customized surgical guides.

To plan a corrective osteotomy, three-dimensional imaging is required, which is most easily obtained with a CT scan with three-dimensional reconstruction. The specific protocol for the CT scan is dictated by the computer software used to plan the osteotomies. The use of computer simulation is often facilitated by an engineer familiar with three-dimensional modeling and surgical planning. Typically, a CT scan is obtained of the bilateral upper extremities, including the joints above and below the deformity, and the images of the unaffected arm superimposed on the affected arm to guide correction. Because the bilateral upper extremities are often affected in Madelung's, the contralateral limb may not provide an acceptable comparison; an age matched normal upper extremity or a more mildly affected extremity may be used for comparison in such cases. Based on this comparative data, osteotomies can be planned that can correct the affected extremity to the normal alignment (Fig. 25.8). Additionally, bone models before and after deformity correction, along with customized guides to assist with the osteotomy and implant placement, can be printed using three-dimensional printing technology and sterilized for use in the operating room.

Corrective osteotomies using three-dimensional modeling are in the early stages of

development and principally have been used to correct post-traumatic deformity. The few case series detailing the use of this technology in Madelung's are promising [37, 38].

Summary

Madelung's deformity is an uncommon congenital condition of the wrist and forearm predominantly presenting bilaterally in adolescent females and may be associated with SHOX deficiency syndromes. Its etiology is incompletely understood. Due to the rarity of this condition, its natural history and the outcomes of surgical treatment are difficult to determine. Surgical intervention appears to improve pain, motion, and the appearance of the wrist, but whether these techniques result in sustained improvements in radiographic alignment is unknown. The risk of recurrence is particularly high in younger children. Moreover, no studies have reported patient reported outcomes to assess the effect of this condition of health-related quality of life or the outcomes of operative management. Future long-term prospective, multicenter studies will improve our ability to care for children with Madelung's deformity.

References

1. Goldfarb CA, Ezaki M, Wall LB, Lam WL, Oberg KC. The Oberg-Manske-Tonkin (OMT) classification of congenital upper extremities: update for 2020. J Hand Surg. 2020;45(6):542–7.
2. Flatt A. The care of congenital hand anomalies. St. Louis: Mosby; 1994.
3. Lecon GD. Leçons Orales De Clinique Chirurgicale: Faites A L'hotel-dieu De Paris, Germer Baillière; 1839, vol. 4; 1834. p. 197.
4. Mostofi SB. Who's who in orthopedics. London: Springer; 2005. p. 89–92, 214, 217–219.
5. Malgaigne JF, Baillière JB. Traité des fractures et des luxations. Paris: chez JB. Baillière; 1855, Vol. 2. Paris; 1855. p. 259–76.
6. Madelung O. Die Spontane Subluxation de Hand Nach Vorne. Verh Dtsch Ges Chir. 1878;7:259–76.
7. Arora AS, Chung KC. Otto W. Madelung and the recognition of Madelung's deformity. J Hand Surg. 2006;31(2):177–82.
8. Vickers D, Nielsen G. Madelung deformity: surgical prophylaxis (physiolysis) during the late growth period by resection of the dyschondrosteosis lesion. J Hand Surg Edinb Scotl. 1992;17(4):401–7.
9. Nielsen JB. Madelung's deformity. A follow-up study of 26 cases and a review of the literature. Acta Orthop Scand. 1977;48(4):379–84.
10. Munns CF, Glass IA, LaBrom R, Hayes M, Flanagan S, Berry M, et al. Histopathological analysis of Leri-Weill dyschondrosteosis: disordered growth plate. Hand Surg Int J Devoted Hand Up Limb Surg Relat Res J Asia-Pac Fed Soc Surg Hand. 2001;6(1):13–23.
11. Seki A, Jinno T, Suzuki E, Takayama S, Ogata T, Fukami M. Skeletal deformity associated with SHOX deficiency. Clin Pediatr Endocrinol. 2014;23(3):65–72.
12. Dawe C, Wynne-Davies R, Fulford GE. Clinical variation in dyschondrosteosis. A report on 13 individuals in 8 families. J Bone Joint Surg Br. 1982;64(3):377–81.
13. Ross JL, Scott Jr C, Marttila P, Kowal K, Nass A, Papenhausen P, et al. Phenotypes associated with SHOX deficiency. J Clin Endocrinol Metab. 2001;86(12):5674–80.
14. Lippe B. Turner Syndrome. Endocrinol Metab Clin N Am. 1991;20(1):121–52.
15. Zinn AR, Wei F, Zhang L, Elder FF, Scott CI, Marttila P, et al. Complete SHOX deficiency causes Langer mesomelic dysplasia. Am J Med Genet. 2002;110(2):158–63.
16. Clement-Jones M, Schiller S, Rao E, Blaschke RJ, Zuniga A, Zeller R, et al. The short stature homeobox gene SHOX is involved in skeletal abnormalities in turner syndrome. Hum Mol Genet. 2000;9(5):695–702.
17. Ghatan AC, Hanel DP. Madelung deformity. J Am Acad Orthop Surg. 2013;21(6):372–82.
18. Rump P, Jongbloed JDH, Sikkema-Raddatz B, Mundlos S, Klopocki E, van der Luijt RB. Madelung deformity in a girl with a novel and de novo mutation in the GNAS gene. Am J Med Genet A. 2011;155A(10):2566–70.
19. Ioan DM, Maximilian C, Fryns JP. Madelung deformity as a pathognomonic feature of the onychoosteodysplasia syndrome. Genet Couns Geneva Switz. 1992;3(1):25–9.
20. Anton JI, Reitz GB, Spiegel MB. Madelung's deformity. Ann Surg. 1938;108(3):411–39.
21. Waters PM, Bae DS. Pediatric hand and upper limb surgery: a practical guide. Philadelphia: Wolters Kluwer Health; 2012.
22. Ducloyer P, Leclercq C, Lisfranc R, Saffar P. Spontaneous ruptures of the extensor tendons of the fingers in Madelung's deformity. J Hand Surg Edinb Scotl. 1991;16(3):329–33.
23. Jebson PJ, Blair WF. Bilateral spontaneous extensor tendon ruptures in Madelung's deformity. J Hand Surg. 1992;17(2):277–80.
24. Shahcheraghi GH, Peyman M, Mozafarian K. Madelung deformity and extensor tendon rupture. Am J Orthop Belle Mead NJ. 2015;44(7):E242–4.

25. McCarroll HR, James MA, Newmeyer WL, Molitor F, Manske PR. Madelung's deformity: quantitative assessment of x-ray deformity. J Hand Surg. 2005;30(6):1211–20.
26. McCarroll HR, James MA, Newmeyer WL, Manske PR. Madelung's deformity: diagnostic thresholds of radiographic measurements. J Hand Surg. 2010;35(5):807–12.
27. Zebala LP, Manske PR, Goldfarb CA. Madelung's deformity: a spectrum of presentation. J Hand Surg. 2007;32(9):1393–401.
28. Peymani A, Dobbe JGG, Streekstra GJ, McCarroll HR, Strackee SD. Quantitative three-dimensional assessment of Madelung deformity. J Hand Surg Eur Vol. 2019;44(10):1041–8.
29. Oishi S, Wheeler L, Ezaki M. Madelung's deformity. In: The pediatric upper extremity. 1st ed. New York: Springer Reference Abzug JM, Kozin S, Zlotolow DA eds. 2015;1763–72.
30. Kozin SH, Zlotolow DA. Madelung Deformity. J Hand Surg. Abzug JM, Kozin S, Zlotolow DA eds. 2015;40(10):2090–8.
31. Otte JE, Popp JE, Samora JB. Treatment of Madelung deformity with Vicker ligament release and radial physiolyses: a case series. J Hand Surg. 2019;44(2):158.e1–9.
32. Del Core M, Beckwith T, Phillips L, Ezaki M, Stutz C, Oishi SN. Long-term outcomes following Vickers ligament release and growth modulation for the treatment of Madelung deformity. J Pediatr Orthop. 2020;40(4):e306–11.
33. Harley BJ, Brown C, Cummings K, Carter PR, Ezaki M. Volar ligament release and distal radius dome osteotomy for correction of Madelung's deformity. J Hand Surg. 2006;31(9):1499–506.
34. Steinman S, Oishi S, Mills J, Bush P, Wheeler L, Ezaki M. Volar ligament release and distal radial dome osteotomy for the correction of Madelung deformity: long-term follow-up. J Bone Joint Surg Am. 2013;95(13):1198–204.
35. Bruno RJ, Blank JE, Ruby LK, Cassidy C, Cohen G, Bergfield TG. Treatment of Madelung's deformity in adults by ulna reduction osteotomy. J Hand Surg. 2003;28(3):421–6.
36. McCarroll HR, James MA. Very distal radial osteotomy for Madelung's deformity. Tech Hand Up Extrem Surg. 2010;14(2):85–93.
37. Bauer AS, Storelli DAR, Sibbel SE, McCarroll HR, Lattanza LL. Preoperative computer simulation and patient-specific guides are safe and effective to correct forearm deformity in children. J Pediatr Orthop. 2017;37(7):504–10.
38. Imai Y, Miyake J, Okada K, Murase T, Yoshikawa H, Moritomo H. Cylindrical corrective osteotomy for Madelung deformity using a computer simulation: case report. J Hand Surg. 2013 Oct;38(10):1925–32.